Proceedings of the
American Control Conference
Baltimore, Maryland • June 1994

Adaptive Speed Control of AC Servo Induction Motors with On-Line Load Estimation

Yee-Pien Yang and Chuan-Feng Fang
Department of Mechanical Engineering
National Taiwan University
Taipei, Taiwan 106, R.O.C.
02-363-0231 Ext.2175 ypyang@w3.me.ntu.edu.tw

Abstract

An adaptive speed control with load torque compensation for ac servo induction motors is proposed. This adaptive control loop that precedes the field oriented control loop consists of a proportional plus integral (PI) controller and a load torque compensator. Their control gains are adjusted adaptively in terms of estimated parameters of an estimation model. The estimation model is a simple first-order predictor with a nonlinear load term, whose parameters are functions of motor time constant, moment of inertia of the rotor, load torque and sampling time of the discrete-time motor model. The total control law is then a combination of the adaptive PI control gain and the load compensation, resulting in a torque command that is fed into the field oriented control loop. Simulation and experimental results show that the proposed adaptive control strategy is robust to the load change and system parameters variation.

1. Introduction

There exist two control loops in the speed control design of an induction motor: the decoupling control loop and the speed regulation loop. The decoupling control loop carries out the field oriented control algorithms, while the speed regulator generates the command torque that is fed into the decoupling loop. Many researchers focused on the design of the decoupling control loop, while staying with a conventional speed regulator with constant PI gains [5, 8]. By linearizing nonlinear motor equations, it is possible to obtain desired performances, such as quick speed response and robustness to the disturbance and system parameters change, around a certain operating point. However, system dynamical parameters and load variations are not perfectly known, and they can vary with the change of environmental temperature, operation condition, process and measurement noises, etc. Particularly, the decoupling control is sensitive to the deviation of rotor resistance. In recent years, various adaptive control technologies have interested many induction motor control designers to improve the robustness of the control system.

The adaptive speed control of induction motors can be classified into two categories: the adaptive flux control [3, 6, 9] and the adaptive speed regulation [1, 4]. The former usually consists of a flux controller and a rotor flux vector estimator in the two-axis decoupling loop, including the generation of the rotor flux reference and the identification of rotor time constant or rotor resistance. Its speed regulation loop is usually a conventional PI controller with constant gains. In contrast, the adaptive speed regulation concerns the adaptive tuning of speed regulator parameters, and its cascade decoupling loop preserves the conventional method through the use of slip frequency control.

The self-tuning regulator addressed in this paper consists of a simple and compact system estimation model for the adaptive speed control of an ac servo induction motor with variable load torques. The estimation model represents system dynamics sufficiently in terms of unknown parameters of various motor constants, viscous friction and load torques. In practice, the load torque occurs often in industrial machine systems [7], and is a major disturbance to the machine system. The adaptive speed regulator is the combination of a PI controller and a load compensator, whose gains are tuned simply according to three parameters estimated adaptively. The three parameters account for all inherent first-order rotor system dynamics, load variation, environmental disturbances, and even nonlinear frictions. Thus, a high rate of parameter estimation convergence and quick, precise speed control can be easily achieved.

2. Dynamical modeling of AC induction motor

The dynamic behavior of a three-phase three-wire induction motor with a Y-type squirrel-cage rotor can be conveniently described by state-space equations in a rotating reference frame. As shown in Fig. 1, the three-phase axes of the stator are denoted by as, bs and cs, respectively, and the stationary reference frame (α, β) is in fixed relation to the three axes, in which the α-axis is assumed to be aligned with the as-axis. Therefore, the angle between the stationary reference frame (α, β) and the synchronously rotating frame (d, q) can be arbitrarily defined, and the flux angle between the flux linkage and the α-axis is denoted by ρ. With sinusoidal supply, the induced rotor current and flux observed on the synchronously rotating frame appear as dc quantities in steady-state conditions.

(1) Electromagnetic circuit dynamics model:

$$\begin{bmatrix} v_{ds} \\ v_{qs} \\ v_{dr} \\ v_{qr} \end{bmatrix} = \begin{bmatrix} R_s + pL_\sigma & -\omega_e L_\sigma & \frac{pM}{L_r} & \frac{-\omega_e M}{L_r} \\ \omega_e L_\sigma & R_s + pL_\sigma & \frac{\omega_e M}{L_r} & \frac{pM}{L_r} \\ \frac{-MR_r}{L_r} & 0 & \frac{R_r}{L_r} + p & -\omega_s \\ 0 & \frac{-MR_r}{L_r} & \omega_s & \frac{R_r}{L_r} + p \end{bmatrix} \cdot \begin{bmatrix} i_{ds} \\ i_{qs} \\ \phi_{dr} \\ \phi_{qr} \end{bmatrix} \qquad (1)$$

where $\omega_s = \omega_e - \omega_r$ is termed the slip speed, and

$$L_\sigma = L_s - M^2/L_r. \qquad (2)$$

(2) Rotor-load dynamics model:

$$\frac{2}{P}(J_m \frac{d\omega_r}{dt} + B_m \omega_r) = T_e - T_L \qquad (3)$$

where the developed torque is

$$T_e = \frac{3}{2}(\frac{P}{2})(\phi_{qr} i_{dr} - \phi_{dr} i_{qr}), \qquad (4)$$

in which

v_{ds}, v_{qs}	stator voltages in field coordinates
i_{ds}, i_{qs}	stator current in field coordinates
i_{dr}, i_{qr}	induced rotor current in field coordinates
ϕ_{qr}, ϕ_{dr}	rotor flux linkages in field coordinates
J_m, B_m	moment of inertia and viscous coefficients of the motor
R_s, R_r	stator resistance and rotor resistance
L_s, L_r	stator and rotor self-inductances
M	mutual or magnetizing inductance
ω_e	stator angular frequency, rad/sec
ω_r	rotor electrical speed, rad/sec
p	=d/dt, differential operator
P	number of poles of the motor
T_e, T_L	electromagnetic and mechanical load torques

The above equations give the complete description of the electromechanical dynamics of an ac induction machine with shorted rotor windings. For a singly fed machine, the voltage v_{dr} and v_{qr} should be assumed as zero.

3. Field oriented control strategy

The field orientation is achieved by adjusting the magnitude and angular frequency of rotor flux vectors. The former is controlled by the primary current and, at the same instant, the latter is tuned synchronously with the primary angular frequency. This control method is called *field oriented* or *vector control* method, in which the ac machine is controlled like a separately excited dc machine in steady-state conditions.

In order to apply the field oriented control, the following conditions must be satisfied by assuming that the drive system operates in steady state:

$$\phi_{dr} = \Phi_0 \quad \phi_{qr} = 0 \quad i_{dr} = 0 \quad i_{qr} = I_0 \qquad (5)$$

The first condition is that the Φ_0-axis should be positioned on the d-axis, whose position is defined by the angle ρ and determined by the combination of the motor rotor angle ρ_r and the slip angle ρ_s, i.e.,

$$\rho = \int \omega_e dt = \rho_r + \rho_s. \qquad (6)$$

The rotor angle can be measured by a position encoder, while the slip angle must be identified accurately during the on-line operation. Moreover, the rotor flux Φ_0 must be constant to satisfy the second condition $i_{dr} = 0$. From Eq. (4) and the third and fourth rows of Eq. (1), the desired decoupling currents in the (d, q) frame and the corresponding slip frequency can be derived as follows:

$$i^*_{ds} = \frac{\Phi_0}{M} \qquad (7)$$

$$i^*_{qs} = \frac{4T^*_e L_r}{3PM^2 i^*_{ds}} \qquad (8)$$

and

$$\omega^*_s = \frac{MR_r}{L_r \Phi_0} i^*_{qs}. \qquad (9)$$

These quantities must be calculated in the field oriented control loop, and used as commands to the power inverter. The torque command T^*_e is generated from a speed regulator by feeding back the rotor electrical speed ω_r. One usually selects the PI controller for speed regulation for its reliable characteristics of robustness and zero steady-state errors in the closed loop. For the ideal state decoupling the developed torque becomes analogous to the DC machine as follows:

$$T_e = \frac{3}{2}(\frac{P}{2})\frac{M}{L_r}\Phi_0 i_{qs}. \qquad (10)$$

4. Adaptive estimation model

The transfer function of Eq. (3) without load disturbance can be written as

$$G(s) = \frac{\omega_r}{T_e}(s) = \frac{P}{2(J_m s + B_m)}. \qquad (11)$$

The discrete-time model can be obtained through a zero-order-hold device as follows:

$$\omega_r(k) + a\omega_r(k-1) = bT_e(k-1) - bT_L(k-1) \qquad (12)$$

where $a = -\exp(-B_m h/J_m)$, $b = (1+a)P/2B_m$ and h is the sampling time. For adaptive control and parameter estimation problems, Eq. (12) is usually expressed in a predictor form:

$$\hat{\omega}_r(k, \theta) = \psi^T(k-1)\hat{\theta}(k-1) \qquad (13)$$

where the regression vector is

$$\psi^T(k-1) = [-\omega_r(k-1) \;\; T_e(k-1) \;\; -1], \qquad (14)$$

and $\hat{\theta}(k)$ is an estimate of system parameter

$$\theta^T = [a \;\; b \;\; c]. \qquad (15)$$

The c, namely the *load parameter*, denotes the load torque bT_L that may vary during the motor control operation.

5. Adaptive Speed Controller

The adaptive controller for the ac servo induction motor consists of an on-line parameter estimator, a PI-based adaptive control loop, and a load torque compensator. The unknown parameter vector θ of the predictor (13) is estimated by the usual recursive least-squares algorithm [2]

$$\hat{\theta}(k) = \hat{\theta}(k-1) + K(k)[\omega_r(k) - \psi^T(k-1)\hat{\theta}(k-1)] \quad (16)$$

$$K(k) = C(k-1)\psi(k-1)[\lambda + \psi^T(k-1)C(k-1)\psi(k-1)] \quad (17)$$

$$C(k) = [I - K(k)\psi^T(k-1)]C(k-1)/\lambda \quad ,0 < \lambda \leq 1 \quad (18)$$

for given initial value $\hat{\theta}(0)$ and $C(-1) = C_0$. To accommodate varying parameters and keep the information content of the estimator constant, the forgetting factor is adjusted as follows [11]

$$\lambda(k) = \frac{1}{2}\{n(k) + \sqrt{n(k)^2 + 4w(k)}\} \quad (19)$$

in which

$$n(k) = 1 - w(k) - e(k)^2/\sigma_0 \quad (20)$$

$$w(k) = \psi^T(k-1)C(k-1)\psi(k-1) \quad (21)$$

where σ_0 is a tuning parameter, and the estimation error is defined as

$$e(k) = \omega_r(k) - \psi^T(k-1)\hat{\theta}(k-1). \quad (22)$$

The conventional digital PI controller is considered for its robust nature. Its transfer function is usually written as

$$G_c(s) = k_p + k_i(\frac{h}{1 - z^{-1}}). \quad (23)$$

The characteristic equation of the closed-loop system without loading becomes

$$z^2 + [a + b(k_p + k_i h) - 1]z - (a + bk_p) = 0. \quad (24)$$

According to the pole placement design method, the closed-loop poles are assigned at $a_1 \pm jb_1$ so that the system has desired rise time and maximum overshoot to a step response. Whenever the parameters $\hat{a}$ and $\hat{b}$ are estimated on-line by Eqs. (16)-(18), the PI gains can be tuned as

$$k_p = -\frac{\hat{a} + a_1^2 + b_1^2}{\hat{b}} \quad (25)$$

$$k_i = \frac{1}{h}(\frac{1 - 2a_1 - \hat{a}}{\hat{b}} - k_p). \quad (26)$$

The total control law is thus a combination of the adaptive PI control gain and the load compensation of the estimate

$$\hat{T}_L = \hat{c}/\hat{b}. \quad (27)$$

The closed-loop scheme of the adaptive controller is shown in Fig. 2.

6. Digital Simulation Study

In the simulations, all the system parameters are the same as those we have in experiments. The sampling time is 0.002 sec. The desired speed control performance is specified so that the closed-loop system has no overshoot and the settling time is 0.3 second for a unit-step command. Therefore, the closed-loop system has a damping ratio of 1 and a undamped natural frequency 20 rad/sec, hence $a_1 = 0.9608$ and $b_1 = 0$.

System parameters are estimated by Eqs. (16)-(18) whenever the motor speed is measured at each sampling instant. The tuning parameter σ_0 in Eq. (20) is 10. The control law is then generated as soon as the PI gains are calculated based on Eqs. (25) and (26) and the load torque is compensated by Eq. (27).

Learning period

We found that a learning period was necessary for the adaptive controller to identify the system parameters before driving the motor to the desired speed. Figure 3 shows that the motor is driven to 500 rpm without learning period. The estimated $\hat{T}_L$ is erroneous before a 2 Nt.m. load is added at the 3rd second, and the estimator is not able to identify the load change. This results in a large oscillation in the motor speed. But when the system is driven with learning as shown in Fig. 4, the adaptive controller is intelligent enough to adapt to load variation with minor disturbance in the motor speed, which is restored in about 0.3 second after the load changes.

In the following simulations, the adaptive controller has learnt system dynamics for 4 seconds, then the system is controlled at zero velocity before the new command is given. However, the covariance matrix C in the recursive least-squares algorithm may become too small to adjust system estimation model to the load change. That means there is much confidence in the current parameters, and thus they tend to change little when new information is coming in. It is then desirable to recover the sensitivity of the estimator by assigning a minimum value, to which C is reset whenever it is smaller.

Covariance resetting

The resetting criterion that works best is to reset the third diagonal element $C(3,3)$ but to maintain other elements of C. This is because the corresponding parameter to $C(3,3)$ is c that accounts for the load variation, while parameters a and b are kept no change for no variation in the machine parameters. The minimum value of $C(3,3)$ is set at 1000 whenever the motor velocity exceeds ± 0.5 rad/sec off the command signal. Figure 5 shows that the estimator updates the load parameter $\hat{c}$, hence $\hat{T}_L$, immediately when a load of 2 Nt.m. is added at the 3rd second and the covariance matrix is reset. The load torque is then compensated accurately so that the motor velocity is restored sooner than the case in Fig. 4 where the covariance matrix was not reset.

7. Experiments

The implementation of the adaptive controller with load torque compensator is set up with an ac servo induction motor IM-408 of Teco Electric & Machinery Co., Ltd., Taiwan. As shown in Fig. 6, the whole control system consists of a

3-phase current-controlled PWM inverter, magnetic powder brake dynamometer, and a 16 bit PC with a 12 bit ADC/DAC card for data translation and conversion. The sampling frequency is 500 Hz.

Covariance resetting and load compensation

Figure 7 shows that $C(3,3)$ is reset as soon as the velocity shifts off its command when the load torque varies, and the velocity response oscillates within 25 rpm off the desired velocity and settles down in half a second. The load compensator obtains a quick and correct information on the estimate $\hat{\theta}$ and then feeds $\hat{T}_L$ to the field oriented control loop in real time (actually there is one sampling-time delay).

8. Summary and Conclusions

This paper provides a simple and efficient method for controlling an ac servo mechanism with viscous friction and time-varying load torque. This method can also be applied to systems with stiction and Coulomb friction, which produce friction torque on the servo system. Further study on the position and torque control of precision mechanisms with various nonlinearities and time-varying dynamics is potentially rewarding.

Acknowledgment

This research was supported by National Science Council under Contract NSC 81-FSP-002-08C and Teco Electric & Machinery Co., Ltd., Taiwan, R.O.C.

References

[1] C. C. Chan, W. S. Leung, and C. W. Ng, "Adaptive Decoupling Control of Induction Motor Drives," *IEEE Trans. Indust. Electronics*, Vol. 37, No. 1, Feb. 1990, pp.41-47.

[2] G. C. Goodwin and K. S. Sin, *Adaptive Filtering, Prediction and Control*, Prentice-Hall, NJ, 1984.

[3] M. Koyama, M. Yano, I. Kamiyama, and S. Yano, "Microprocessor-Based Vector Control System for Induction Motor Drives with Rotor Time Constant Identification Function," *IEEE Trans. Indust. Appl.*, Vol. IA-22, No. 3, May/June 1986, pp.453-459.

[4] C. M. Liaw, C. T. Pan, and Y. C. Chen, "An Adaptive Controller for Current-Fed Induction Motor," *IEEE Trans. Aerosp. Elect. Syst.*, Vol. 24, No. 3, 1988, pp. 250-262.

[5] R. Marina, S. Peresada, and P. Valigi, "Adaptive Input-Output Linearizing Control of Induction Motors," *IEEE Trans. Auto. Contr.*, Vol. 38, No. 2, Feb. 1993, pp.208-221.

[6] H. Sugimoto and S. Tamai, "Secondary Resistance Identification of an Induction Motor Applied Model Reference Adaptive System and Its Characteristics," *IEEE Trans. Indust. Appl.*, Vol. IA-23, No. 2, 1987, pp.296-303.

[7] J. L. Stein and C. H. Wang, "Analysis of Power Monitoring on AC Induction Drive Systems," *Trans. ASME, J. Dyn. Syst., Meas., and Contr.*, Vol. 112, June 1990, pp.239-247.

[8] A. Teel, R. Kadiyala, P. Kokotovic, and S. S. Sastry, "Indirect Techniques for Adaptive Input-Output Linearization of Nonlinear Systems," *Int. J. Contr.*, Vol. 53, 1991, pp.239-247.

[9] C. Wang, D. W. Novotny, and T. A. Lipo, "An Automated Rotor Time Constant Measurement System for Indirect Field Oriented Drives," *IEEE Trans. Indust. Appl.*, Vol. 34, No. 1, 1988, pp.151-159.

[10] Y. P. Yang and J. S. Chu, "Adaptive Velocity Control of DC Motors with Coulomb Friction Identification," *Trans. ASME, J. Dyn. Syst., Meas., and Contr.*, Vol. 115, March 1993, pp.95-115.

[11] B. E. Ydstie, L. S. Kershenbaum, and R. W. H. Sargent, " Theory and Applications of an Extended Horizon Self-Tuning Controller," *AIChE J.*, Vol. 31, November 1985, pp.1771-1780.

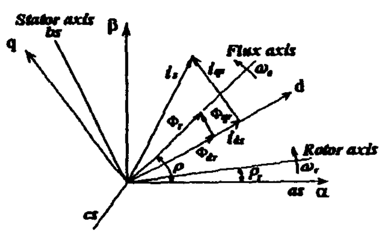

Fig. 1: Phasor diagram of the field orientation control

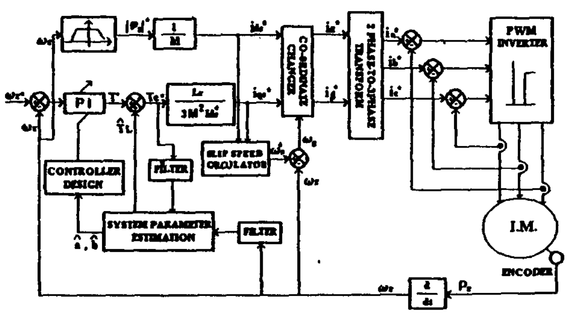

Fig. 2: Adaptive velocity control of ac servo induction motor with load compensation

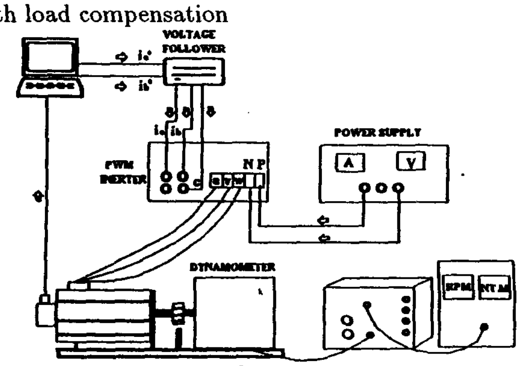

Fig. 6: The experimental setup

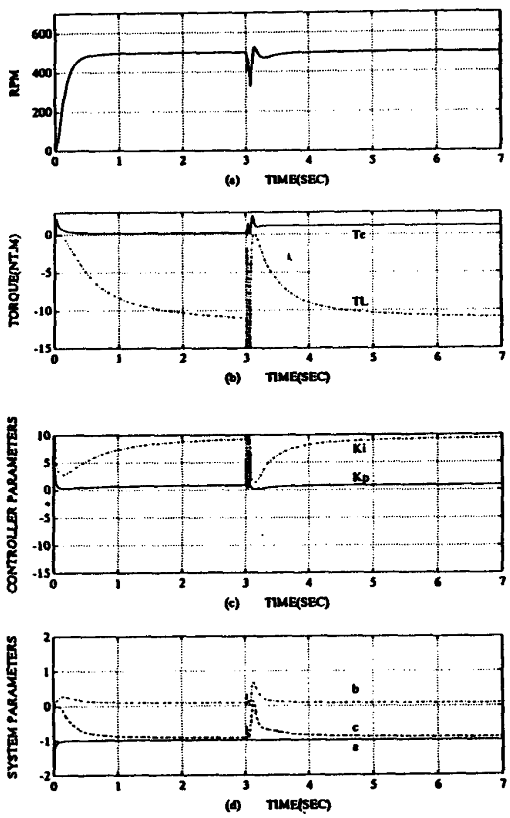

Fig. 3: Velocity control with load disturbance, no learning period

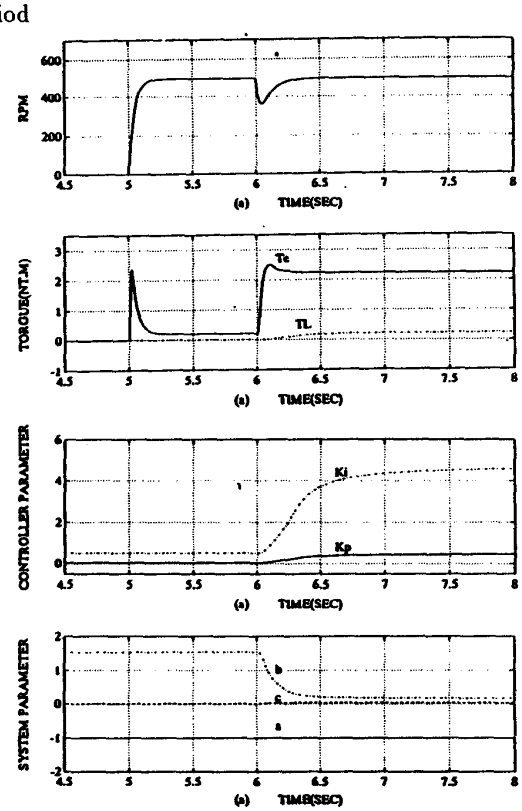

Fig. 4: Velocity control with load disturbance after learning

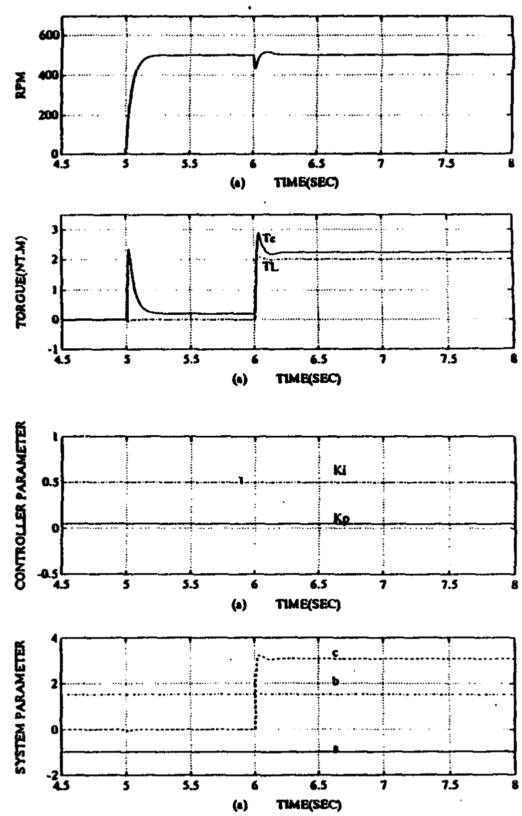

Fig. 5: Velocity control with load disturbance after learning and covariance matrix resetting

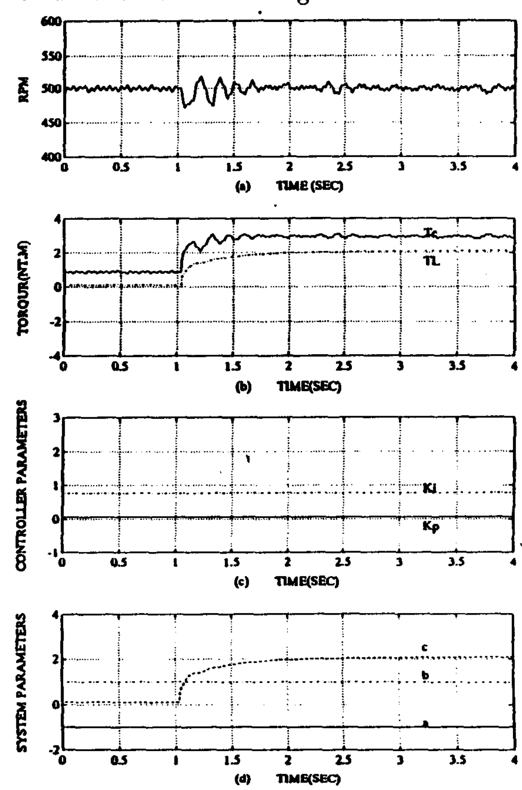

Fig. 7: Velocity control under load disturbance